生物生産施設環境(J. Bio. Fac. Env.) 1(1) : 72-83, 1992

An Application of k-ε Turbulence Model to Predict How a Rectangular Obstacle with Heat Flux Affects Air Flow in An Experimental Animal House

Choi, Hong-Lim and Kim, Hyeon-Tae

Dept. of Agr. Eng., Gyeongsang Nat'l Univ., Jinju 660-701

實驗畜舍의 空氣流動豫測을 위한 k-ε 亂流模型 適用

崔弘林 · 金鉉台

경상大學校 農工學科

摘 要

우리 나라 축사는 생산효율 提高를 위하여 대형화, 밀폐화, 고밀도화, 자동화 경향이 뚜렷하다. 대형의 밀폐된 고밀도 축사는 쾌적한 실내환경을 前提로 하기 때문에 기계적으로 실내환경을 적절히 制御하지 않으면 안된다. 制限된 공간에 먼지, 병원성 미생물, 유해기체, 수분이나 열의 과도한 集積은 생산과 재생산효율에 심각한 영향을 미친다. 그러므로 축사내 生産主體인 가축과 작업인이 쾌적한 실내환경에서 생산활동을 할 수 있도록 熱的, 化學的/生物學的 환경을 물리적으로 제어하지 않으면 안된다.

본 연구는 실험축사내 가축이 일정한 熱을 발생할 때 실내공기의 流動형태를 예측하기 위해서 수행하였다. 이 연구의 결과를 실내환경제어를 위한 환기시스템 策略 開發의 기초자료로 활용할 수 있다. 실험축사내의 공기유동을 예측하기 위해 Body-Fitted Coordinate(BFC)의 격자배열과 k-ε 난류모형 및 SIMPLE 계열 solution scheme을 사용하였으며, 예측의 有效性 검정은 Boon (1978)의 실험결과를 이용하였다. 예측한 공기유동의 형태와 실험한 공기유동의 형태를 비교한 결과 대체로 만족할만한 결과를 얻었다. 그러나 유입공기의 온도가 10℃인 경우의 공기유동은 실험유동형태와 약간의 차이가 있었다. 즉, 실험에서는 수평슬롯으로 유입된 공기가 바로 아래로 굴절되어 流動하였으나, 예측의 결과는 일정 거리로 수평방향으로 유동하다가 아래로 굴절하였다. 이런 유동의 차이는 k-ε 亂流모형 自體가 경험적으로 浮力에 민감하게 반응않는 결함이 원인이 될 수도 있으며, 실험의 부적절한 수행이 원인이 될 수도 있다. 이 流動의 경우 Reynolds 數가 3,000정도의 亂流이며, 完全發達流動 (fully-developed flow)이므로 慣性力 (inertia force)이 浮力 (buoyancy force)보다 커, 일정거리 수평으로 유동하다가 아래로 굴절할 수도 있기 때문이다. 앞으로 이를 규명하기 위한 보다 깊이있는 연구가 이루어져야 할 것이다.

Introduction

Introduction The rapid rise of the value of land and wages has led to the development of a livestock industry which relies on more confined methods of production. Since improper indoor environment lowers the efficiency of production and reproduction of animals in a confined livestock building (Hellickson & Walker, 1983 ; Choi, 1989), it becomes more necessary to provide optimum indoor environment for animals and workers.

Generally temperature, humidity, contaminants (dust and harmful gases) are known as major environmental parameters controlled. Barber(1981) concluded that mechanical ventilation is a practically acceptable medium to dilute contaminants in a confined

livestock building. A typical ventilation graph based on temperature and humidity and a conceptually new ventilation graph including additional parameters for determining the ventilation rate can be referred to Albright(1991), ASHRAE(1989), and Hellickson& Walker(1983). These references deals with ventilation in quantity.

It often happens that incoming air is exhausted to outlet without mixing with existing indoor air (by-passing or short-circuiting) or air speed reaches almost zero in some regions(dead zone or stangnant zone) so that ventilation air flow does not dilute effectively contaminants in a building. Determining the ventilation rate based on the ventilation graphs is necessary but not sufficient. Therefore a quantitative study should go along with a qualitative study to confirm the effectiveness of the ventilation system for a livestock building (Albright, 1984). A qualitative study includes predicting scalars (temperature, humidity and contaminants) distributions in a ventilated building, of which motion is determined by air flow. Therefore it is important to explore air flow patterns in a livestock building, which provides basic information for optimum design of the ventilation system.

A research group of NIAE in U.K. has conducted extensive experimental work on air flow pattern in a full-scale livestock building. Carpenter et al. (1972), Randall (1975), Randall and Battams (1976), Boon (1978), Capenter and Moulsely (1978), Randall and Battams (1979), Randall (1980), Boon (1984) visualized air flow patterns for various flow configurations in a livestock building ; the effect of building layout, the effect of ambient temperature, and the effect of internal obstruction. Some of their work studied the stability of air flow and its creteria.

However, since the adjustment of the parameters of structure and ventilation system is both difficult and expensive for a full-scale structure, it is not readily adaptable for prediction of air movement in a livestock builiding. This is the major shortcoming of experimental work.

Timmons (1979) employed fluid dynamic theory in simulating air flow motion in a ventilated space to overcome the limitation of experiment. He formulated the modified inviscid Navier-Stokes equations with the Z-ω method to simulate overall air flow patterns, which has not been often used due to its serious shortcomings. Choi et al.(1988, 1990) applied the k-ε turbulence model for calculation of air velocities in a ventilated enclosure with and without internal obstruction.

The work presented in this article was to investigate the effects of buoyancy force to air flow, created by the temperature difference between the temperature of entering air jet and that of the simulated pigs, and the effects of obstruction ; pigs and solid walls, using a modified version of the TEACH-like computer program for steady-state, two dimensional, non-isothermal, and recirculating flow in a ventilated livestock building.

Mathermatical Model

1. Turbulence model (two-equation model : k-ε model)

Since Air motion in a livestock building is bascially turbulent flow, the the terms created in derivation of the governing equations for turbulent air motion should be quanitified. The oldest proposal for modeling the turbulent stresses, $-\rho\langle u_i u_j \rangle$ turned out to become a significant part of most turbulence models of practical use today. Boussinesq's eddy-viscosity concept which assumes that, in analogy to the viscous stresses in laminar flows, the turbulent stresses are proportional to the mean-velocity gradients. For general flow situations, this concept may be expressed as :

$$-\rho\langle u_i u_j\rangle = -\mu_t \left(\frac{\partial U_i}{\partial x_j} + \frac{\partial U_i}{\partial x_i} \right) - 2/3\,\rho\, k\, \delta_{ij} \quad (1)$$

Turbulent viscosity(μ_t), in contrast to the molecular viscosity(μ), is not a fluid property but depends strongly on the state of turbulence. Turbulence is assumed to be characterized by the turbulent kinetic energy, k, and its dissipation rate, ε, known as the twoequation turbulence model. Turbulent viscosity

is determined by local values of k and ε.

$$\mu_t = C\mu \cdot \rho \frac{k^2}{\varepsilon} \quad (2)$$

2. Governing epuations

Air motion in a livestock building is bascially turbulent flow, which is governed by the the law of mass conservation, momentum conservation, and energy conservation. The governing differential equations of turbulent flow take the following forms for steady-state, two dimensional, non-isothermal mean flow. The equations are expressed in the Body-Fitted Coordinate(BFC) system, discussed more in the Body-Fitted Coordinate system.

1) Continuity :

$$\frac{\partial}{\partial x}(\rho U) + \frac{\partial}{\partial x}(\rho V) = 0 \quad (3)$$

2) U-momentum equation :

$$\frac{\partial}{\partial x}(\rho U^2) + \frac{\partial}{\partial y}(\rho UV) = -\frac{\partial P}{\partial x} + \frac{\partial}{\partial x}\left(\mu_{eff}\frac{\partial U}{\partial x}\right) + \frac{\partial}{\partial y}\left(\mu_{eff}\frac{\partial U}{\partial y}\right) + S_u \quad (4)$$

where, $S_u = \frac{\partial}{\partial x}\left(\mu_{eff}\frac{\partial U}{\partial x}\right) + \frac{\partial}{\partial y}\left(\mu_{eff}\frac{\partial U}{\partial y}\right)$

3) V-momentum equation :

$$\frac{\partial}{\partial x}(\rho UV) + \frac{\partial}{\partial y}(\rho V^2) = -\frac{\partial P}{\partial y} + \frac{\partial}{\partial x}\left(\mu_{eff}\frac{\partial V}{\partial x}\right) + \frac{\partial}{\partial y}\left(\mu_{eff}\frac{\partial V}{\partial y}\right) + \rho_r g\beta(T-T_r) + S_v \quad (5)$$

where, $S_v = \frac{\partial}{\partial x}\left(\mu_{eff}\frac{\partial V}{\partial x}\right) + \frac{\partial}{\partial y}\left(\mu_{eff}\frac{\partial V}{\partial y}\right)$

4) Energy transport equation :

$$\frac{\partial}{\partial x}(\rho Uh) + \frac{\partial}{\partial y}(\rho Vh) = \frac{\partial}{\partial x}\left(\gamma_{eff}\frac{\partial h}{\partial x}\right) + \frac{\partial}{\partial y}\left(\gamma_{eff}\frac{\partial h}{\partial y}\right) + S_h \quad (6)$$

where, S_h : source terms like heat flux

5) Turbulent kinetic energy equation (k-equation) :

$$\frac{\partial}{\partial x}(\rho Uk) + \frac{\partial}{\partial y}(\rho Vk) = \frac{\partial}{\partial x}\left(\frac{\mu_{eff}}{\sigma_k}\frac{\partial k}{\partial x}\right) + \frac{\partial}{\partial y}\left(\frac{\mu_{eff}}{\sigma_k}\frac{\partial k}{\partial y}\right) + G - C_D\rho\varepsilon + G_B \quad (7)$$

where, $G = \mu_t\left[\{2(\frac{\partial U}{\partial x})^2 + (\frac{\partial U}{\partial x})^2\} + (\frac{\partial U}{\partial y} + \frac{\partial V}{\partial x})^2\right]$;

$G_B = \beta g\left(\frac{\mu_t}{\sigma_t}\right)\frac{\partial \theta}{\partial y}$: $\theta = T - T_r$

6) Dissipation rate of turbulent kinetic energy (ε-equation) :

$$\frac{\partial}{\partial t}(\rho\varepsilon) + \frac{\partial}{\partial x}(\rho U\varepsilon) + \frac{\partial}{\partial y}(\rho V\varepsilon) = \frac{\partial}{\partial x}\left(\frac{\mu_{eff}}{\sigma_e}\frac{\partial \varepsilon}{\partial x}\right) + \frac{\partial}{\partial y}\left(\frac{\mu_{eff}}{\sigma_e}\frac{\partial \varepsilon}{\partial y}\right) + \frac{\varepsilon}{k}(C_1G - C_2\rho\varepsilon) + C_3\frac{\varepsilon}{k}G_B \quad (8)$$

Table. 1. Value of constants in the turbulence model

C_μ	C_D	C_1	C_2	C_3	σ_k	σ_e
0.09	1.0	1.44	1.92	1.0	1.0	1.3

Numerical Analysis 1.

1. Grid generation for body-fitted coordinates

1) Equations

In general, grid generation is a mapping between a physical space and a computational space. The transformation is given by the functions

$$\xi = \xi\ (x,y) \tag{9a}$$

$$\eta = \eta\ (x,y) \tag{9b}$$

where ξ and η represent coordinates in the transformed computational plane in Fig.1.

In this method employed in the grid generation program reported here, the generating functions are either Lapalce equations or Poission equations. Use of the Laplace equations yields

$$\xi_{xx} + \xi_{yy} = 0 \tag{10a}$$

$$\eta_{xx} + \eta_{yy} = 0 \tag{10b}$$

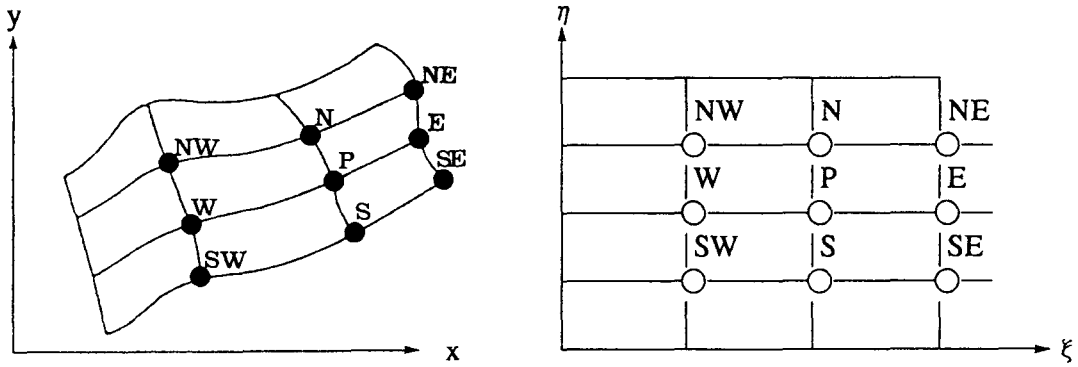

a. Physical plane

b. Computational plane

Fig. 1. Mapping from physical plane to computational plane

Solution of this set of equations will result in a grid system with maximum orthogonality of the grid lines, but the grid line spacing will be as unifrom as possible. There is no way to control the spacing of interior points. In order to cluster grid points or lines spacing, it is necessary to incorporate control functions (P, Q) into Eq. (11) and (12). This results in a Poisson equation for the transformation.

$$\xi_{xx} + \xi_{yy} = P\ (\xi,\eta) \tag{11a}$$

$$\eta_{xx} + \eta_{yy} = Q\ (\xi,\eta) \tag{11b}$$

2) Discretization of the Equations

The Laplace euqations (10a, b) can be transformed to the computatioal plane, resulting in two elliptic equations in the form

$$\alpha x_{\xi\xi} - 2\beta x_{\xi\eta} + \gamma x_{\eta\eta} = 0 \tag{12a}$$

$$\alpha y_{\xi\xi} - 2\beta y_{\xi\eta} + \gamma y_{\eta\eta} = 0 \tag{12b}$$

$$\text{where, } \alpha = x_\eta^2 + y_\eta^2 \ ; \ \beta = x_\xi x_\eta + y_\xi y_\eta \ ; \ \gamma = x_\xi^2 + y_\xi^2 \tag{12c}$$

3) Soution procedure

Rearrangement of Eq.(10) for finite difference form of the x-equation yields xP at the grid locations shown in Fig.1b.

$$x_P = \frac{a_N x_N + a_S x_S + a_E x_E + a_W x_W + S_U}{a_N + a_S + a_E + a_W - S_P} \tag{13a}$$

$$\text{where, } S_U = B/2(x_{NE} - x_{NW} + x_{SW} - x_{SE}) \tag{13b}$$

$$S_P = 0 \tag{13c}$$

The convergence criterion for the overall solution procedure consists of a user-specified reduction in the sum of the residuals of the euqations. At the iteration a residual is calculated at each point according to :

$$\varepsilon = \frac{a_N x_N + a_S x_S + a_E x_E + a_W x_W + S_U}{a_N + a_S + a_E + a_W - S_P} - x_P \tag{14}$$

2. Formulation of discretizde equations

Eq. (3)~(8) can be discribed by the differential equations of the form for single phase flow. $\phi = 1$ yields the continuity equation.

$$\frac{\partial}{\partial t}(\rho\phi) + \nabla(\rho\phi V) - \nabla(\Gamma_s \nabla\phi) = S_s \tag{15}$$

The values of the flow variables at each cell and for each time-step are the sought-for outcome of the compuatation. Fig.1a is the control voulme for scalar

and (b) for velocities. The code uses the staggered-grid arrangement (Fig. 1b), in which the location of the velocity nodes is displaced with respect to the location of the node used for other scalar variables, and located on the cell faces. The benefits of this arrangement are that each velocity component is driven by two adjacent pressures and the value of the velocity is avaiable, without interpolation, at the cell face, where it will be needed to computer the convection fluxes into cell.

The results of the intergration process can be grouped into an equation of the form

$$a_P\phi_P = a_N\phi_N + a_S\phi_S + a_E\phi_E + a_W\phi_W + a_T\phi_T + b \quad (16)$$

where, $a_E = \rho A_E [-U_e] + D_E$, for example.

$a_T = (V_P/\triangle t)\,\rho_T$

$b = V_P C\phi_P V\phi_P$

Eq.(16) can be rewritten for ϕP as :

$$\phi_P = \frac{a_E\phi_E + a_W\phi_W + a_N\phi_N + a_S\phi_S + a_T\phi_T + b}{a_E + a_W + a_N + a_S + a_T + a_P} \quad (17)$$

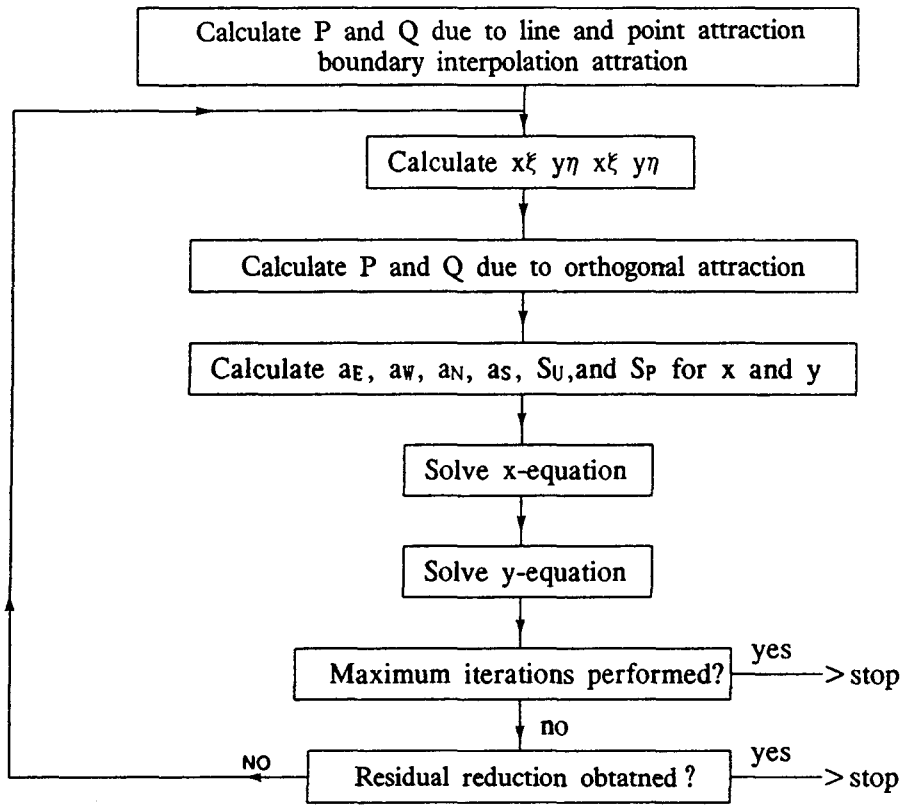

Fig. 2. Solution procedure

the cell faces. The benefits of this arrangement are that each velocity component is driven by two adjacent pressures and the value of the velocity is avaiable, without interpolation, at the cell face, where it will be needed to computer the convection fluxes into cell.

The results of the intergration process can be grouped into an equation of the form :

$$a_P\phi_P = a_N\phi_N + a_S\phi_S + a_E\phi_E + a_W\phi_W + a_T\phi_T + b \quad (16)$$

where, $a_E = \rho A_E [-U_e] + D_E$, for example.

$a_T = (V_P/\triangle t)\,\rho_T$

$b = V_P C\phi_P V\phi_P$

Eq.(16) can be rewritten for P as in Eq.(17) and solved by staggered grid system shown in Fig.3.

$$\phi_P = \frac{a_E\phi_E + a_W\phi_W + a_N\phi_N + a_S\phi_S + a_T\phi_T + b}{a_E + a_W + a_N + a_S + a_T + a_P} \quad (17)$$

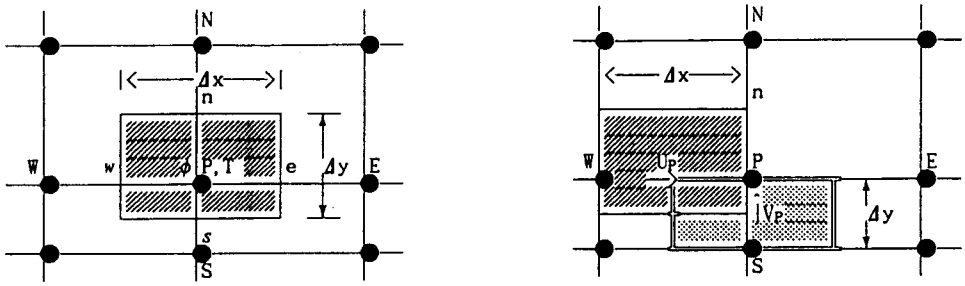

Fig. 3. Two dimensional calculation domain for (a) scalar (b) U-velocity(▨), V-velocity(▩) in computational plane.

3. Linerization of source term

When the source term S depends on ϕ, the dependence can be linearized by Eq.(18). This is done because our nominally linear framework would allow only a formally linear dependence, and the incorporation of linear dependence is better than treating S as a constant.

$$S = S_C + S_P\phi_P \quad (18)$$

SC includes in b, and -SP in ap in Eq.(16).

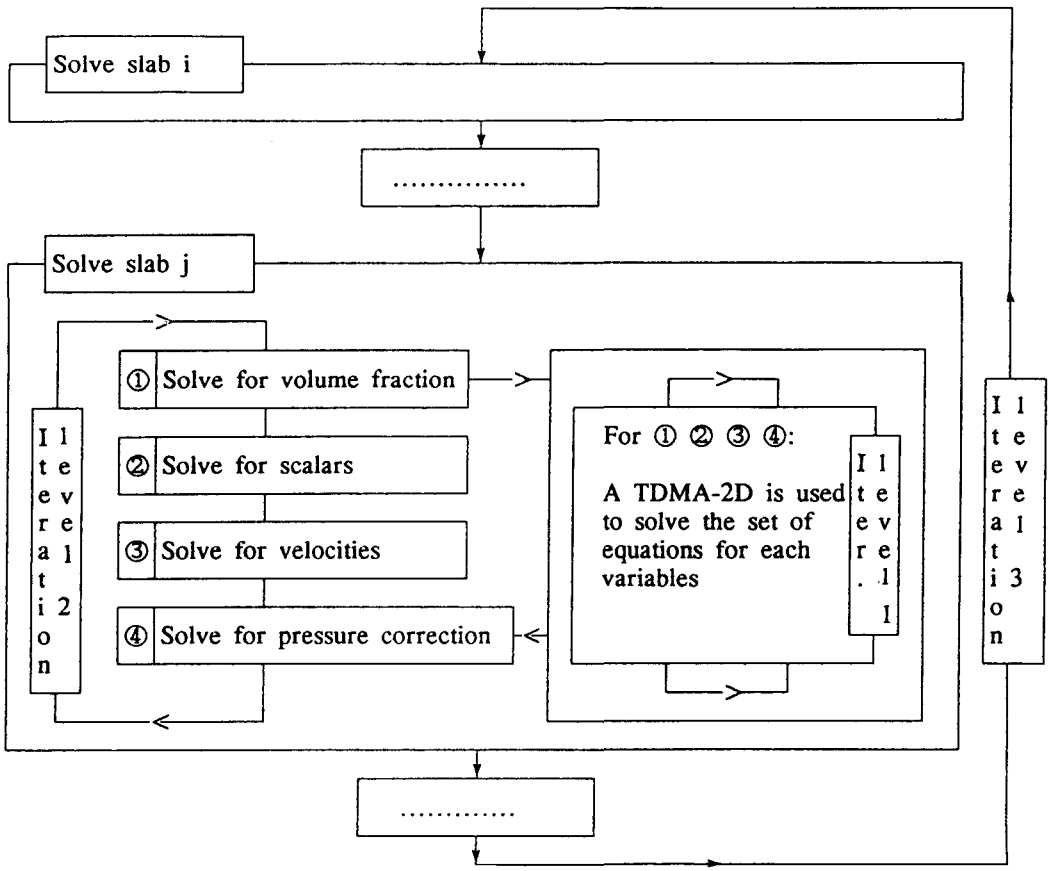

Fig. 4. Solution algorithm for two dimensional discretized equations.

4. SIMPLE-like algorithm

The solution algorithm is a marching one, that sweeps the domain in a slab-by-slab fashion. A slab is an X-Y plane of cells, and contains NX * NY cells. The code has three levels of iteration. The iternation level 1 in Fig. 2 the NX * NY system of equations for a variable ϕ at each slab, using either a generalized 2D version of the well-known Tri-Diagonal Matrix Algorithm (TDMA) or a Jacobi point by point procedure. The iteration level 2 has to blend together the changes effected for each variable separately. The pressure/velocity linkage has also to be dealt with this level. The pressure field has to be such that the velocities resulting from the momentum equations verify the continuity equation.

The iteration level 3 repeatly solve the equations for all variables including pressure correction updating the corrections between them. In the slab by slab procedure, the off-slab values are assumed known, whereas they are not. As a consequence, the solution for the current slab is not the final one, and the solution procedure has to sweep all the slab in the domain several level.

Result and Discussion

Air flow patterns in Fig. 6a~ Fig. 10a were visualized by Boon(1978), using liquid film bubbles in the flow. Fig. 6a~ Fig. 10a were used to examine the ability of the simulation model applied in predicting a realistic air flow.

1. Experimetal procedure

The full-scale section of a livestock building used for calculation geometry, Fig. 5, in this work was described in detail in Boon(1978). The section was 7.80m wide representing a typical span which may accomodate two pig pens and three passages. It was arranged with solid walls, 1.05m high, to form a feeding passage at each side and with a central wall to form two pens. The outlay of the experimental livestock building is shown in Fig. 6 with the presence, and Fig. 7 with the absence of solid walls. The depth of the section represented the length of one pen and the height was 1.87m to the eaves and 2.43m to the ridge. An insulated shell connected to an air conditioner and enclosing the side walls and roof allowed the temperature outside the section to be controlled. Ventilating air was

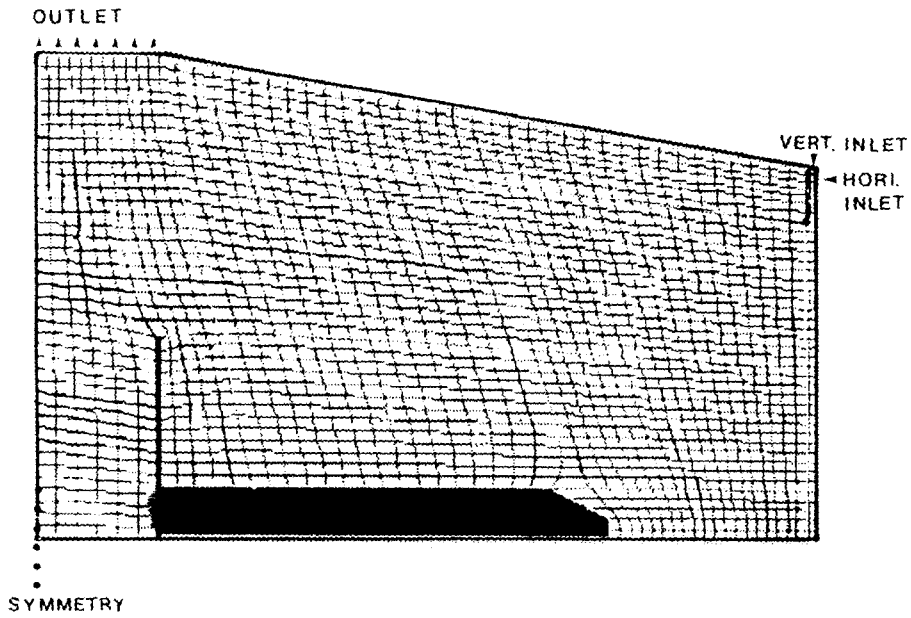

Fig. 5. Calculation domain with Body-Fitted Coordinate system

exhausted from the shell by a 0.457m propeller fan was mounted 0.45m above the ceiling in a vertial duct. Heat released from the stock resulted from 26 large white pigs, 13 in each pen, generating heat 170W/m^2 for 10℃, 130W/m^2 for 17℃. The air inlet was a 0.041m wide slit, the full length of the building section, near the top of each side wall 1.70m from the floor. Approximately 0.52m^3/s for inlet air temperature of 17℃ and 0.16m^3/s for 10℃. The outlet was 0.52m^2 aperture in the center of the apex of the roof.

2. Air flow patterns

1) The effect of obstruction

The inlet air jet enters horizontally in flow configurations of Fig. 6 and Fig.7 with the entering air temperature of 17℃ (equivalent to Arichimedes number of 1.25E-4) and Reynolds number of 10,000. The only difference in the flow configurations is the presence of physical obstruction. Overall similarities were perceived between the calculated and the observed air flow in Fig. 6 and Fig. 7. No distinct difference of air motion is observed in Fig. 6a and in 〈Fig. 7a〉 either with or without internal obstacles. There is, however, some difference in the size of a primary recirculation flow. Boon's observation do not show the details of air motion and the magnitude of air velocities, but calculations in this work, reveal such details Fig. 6b and Fig. 7b. The more detailed air motion in this work provides additional information.

The calculated air flow of Fig. 6b with the presence of an obstacle shows primary recirculation in the center of the space ; it rotates counterclockwise and is squeezed due to the solid wall. A seconadry recirculation flow is observed between the symmertric line and the internal solid wall, which separates the passage and the pig pen. Initially a free air jet in 〈Fig. 6b〉 deflects upwards and attaches to the ceiling due to Coanda effect. The reattached flow becomes a wall jet and continues to move along the ceiling. The solid wall creates a dominating adverse pressure gradient, which leads to flow separartion. A weak eddy is also observed in the lower right corner of Fig. 6b.

The physical obstructions in Fig.6 modifies air flow significantly. They deflect air flow and lead to flow separations by creating adverse pressure gradient, and dissipates the turbulent kinetic energy of the air flow. In most cases, physical obstructions adversely effect to air flow. However, they purposefully were utilized to redirect or to decelerate air flow. As shown in Fig. 6b, air velocities are relatively smaller, compared to those of Fig. 7b. In paricular, the air velocities approaches zero at the height of animals while those in other regions has larger velocities. Except in cold winter, it is desirable to have higher air velocities to maintain proper indoor thermal and chemical environments.

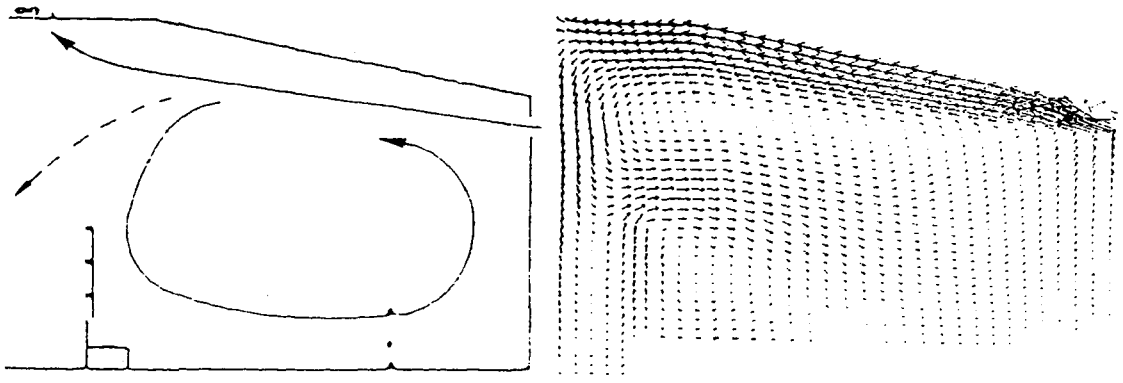

(a) (b)

Fig. 6. a) The observation by Boon(1978) b) The calculated flow patterns

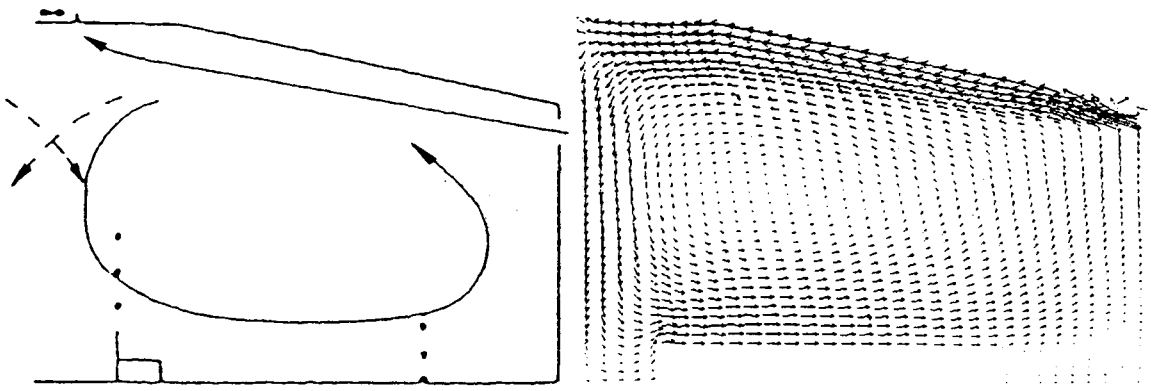

(a) (b)

Fig. 7. a) The observed by Boon(1978) b) The calculated flow patterns

Short-circuiting phenomenum is observed in the flow configuration of Fig. 6 and Fig, 7. Much of the entering air flow through the slot inlet at eave are exhaused by the fan at the ridge. A recirculating air forms a primary flow with lower velocity, so with lower momentum, rotates counterclockwise, and it again separates at the top of the internal solid wall. Some of them are entrained by the inlet air jet, and the rest forms the secondary eddy rotates clockwise in the region between the internal solid wall and the inlet wall. Basically, air flow with less momentum has less ability in diluting contaminants. Excessive harmful gases or dust may accumlulate on the pigs or on the floor since the overall velocity is much smaller in the flow field.

2. The effect of ambient temperature

To see the effect of thermal buoyancy force on air flow, the entering air temperature of 10℃ was applied to the flow geometry of Fig. 8 with heat flux of 170 W/m^2, released from real pigs at floor (equivalent to Archimedes number of 8.95E-3) and Reynolds number of 3E+3. The calculated air flow in Fig. 8b moves forwards, and falls down in the middle of the space and rotates clockwise. This may indicate that that buoyancy force overcomes inertia force. However, the observed air flow in Fig. 8a falls down immediately after entering, and rotates counter-clockwise. Perhaps discrepancy of the observed in Fig. 8a and the calculated air flow in 〈Fig. 8b〉 originated from the insensiti-

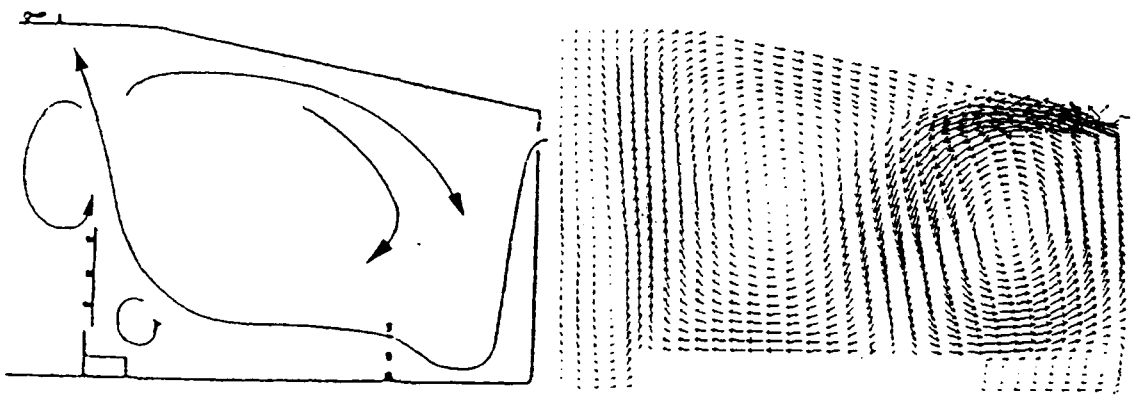

(a) (b)

Fig. 8. a) The observed by Boon(1978) b) The calculated flow patterns

vity of the k-ε turbulence model itself to buoyancy, based on experience, or from improper management of experiment. Since the flow is a fully-developed and a turbulent flow, the inertia force may overcome buoyancy force to some distance from the inlet.

If such a ventilation system is adapted in cold winter, it may create a problem. When a very cold air jet drops on the head of animals, it causes a chilly draft to the animals. It is recommended to direct air flow downward so that the cold jet gets warmer along the inside wall.

3. The effect of direction of inlet air jet

A typical ventilation system in a cold winter directs entering air jet downwards, and moves along the wall so the air gets warmer to avoid draft to animals. Fig. 9b shows a flow pattern for the vertical inlet air flow with temerature of 17℃ and Reynolds number of 1E+4. It is expected the inertia force of the flow is predominant. As shown in Fig. 9b, A strong air jet rotates clockwisely and impinges an obstacles which prevents air flow from diffusing to the left-half of the space. A primary recirculation flow rotates clockwise and attaches to the roof and separates. Someof them forms a secondary recirculation flow in the left-half region of the space, and much is entrained by an inlet air jet, due to strong adverse pressure gradient. Small eddies can be observed in the upper-left corner of the obstacle, similar with the observed in Fig. 9a, and in the lower region between the symmetric axis and the solid wall. A major concern in Fig. 9b is the discrepancy of the magnitude of air velocities between the right-half and the left-half is so large that much of the secondary flow in the left-half region of the space is exhaused to outlet. The left-half region can be considered to as a stagnant region. The ventilation system can not dilute contaminants due to incomplete air mixing. The size of recirculation flows in Fig. 9b is much different from those in Fig. 9a. This may be caused by improper reflection of real pigs beavior laying at the floor to boundary condition in the calculation, which is referred to as an obstacle ; sometime pigs in the pen move around, or by the insenstivity of the k-ε turbulence model to buoyancy.

The observed air flow for Fig. 9 with Ar=2.64E−4 and Re=1E+4, and the air flow for Fig. 10 with Ar=8.95E−2 and Re=3E+3 are basically same as the calculated.

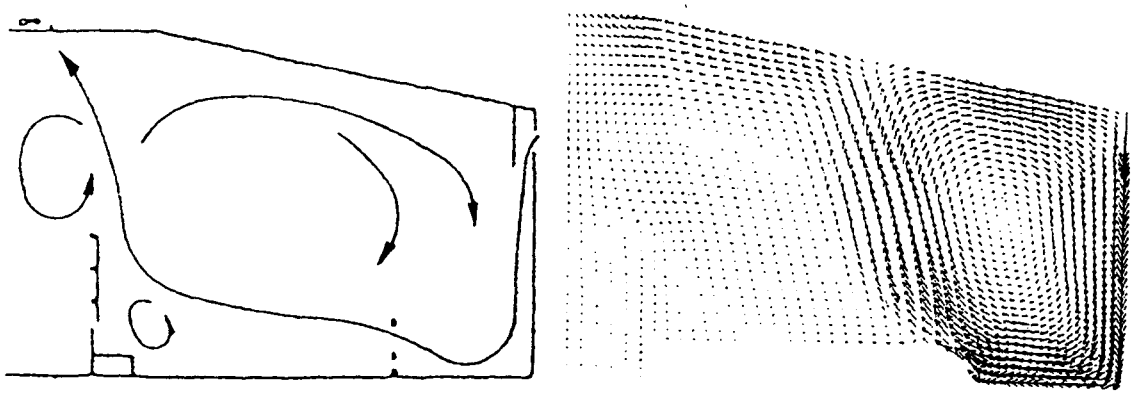

(a) (b)

Fig. 9. a) The observed by Boon(1978) b) The calculated flow patterns.

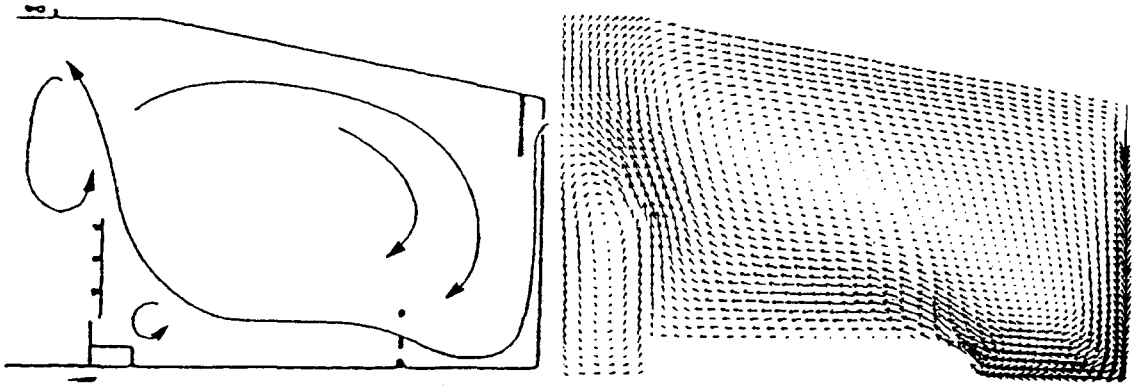

(a) (b)

Fig. 10. a) The observed by Boon(1978) b) The calculated flow patterns

Conclusion

The TEACH-like program, which uses the k-ε turbulence model, was applied to a ventilated air space having obstructions ; 26 real pigs with heat flux of 130 W/m² for inlet temperature of 17℃ and Reynolds number of 1E+4, and 170W/m² for 10℃ and Re of 3E+3. Results were compared to experimental data and the following conclusions were drawn.

1. It is possible to predict, with reasonable accuracy, overall flow patterns and temperature distribution in a ventilated space, represneting a typical livestock building having phyical obstructions, by solving dis- cretized conservation equations and using the standard k-ε model.

2. Obstructions in a ventilated space significantly modifies air flow and/or creates dead regions. The obstacle like the real pigs in the geometric configuration of Fig. 9b dissipates most kinetic energy of the air jet due to impingement, which eventually leads to imcomplete mixing due to lack of momentum of the flow. It should avoid the obstruction in the route of the inlet air jet flow since the inlet jet governs the whole flow field.

3. The ventlation system, having inlets at the eaves and outlet at ridge leads air flow short-circuited. Such a system lowers the effectiveness so that it is easy to create the dead regions.

4. The buoyancy force orginated from the temperature difference between the entering air and the heat flux from the real pigs moves air flow upwards. Heat accumulation can be observed in the stagnant region created by obstructions.

5. It is prerequiste to simulate air flow and temperature distributions in a ventilated space for design purpose to evaluate the efficiency of the ventilation system to be condstructed.

〈Symbols〉

- $a's$: coefficents in finite-domain equation in Eq. (16)
- b : source term of ϕ in Eq.(16)
- U : Horizontal mean velocity
- V : Vertical mean velocity
- k : turbulent kinetic energy
- ε : the rate of dissipation of turbulent kinetic energy
- h : enthalpy
- S : a source term in Eq.(18)
- ρ : density
- α : upwinding-scheme control parameter
- β : coefficient of gas expansion
- C_μ : coefficient
- μ_{eff} : effective turbulent viscosity
- μ : laminar viscodity
- σ : laminar Prandtl (Pr) number
- σ_t : turbulent Prandtl number
- ϕ : varaibles in question in Eq.(15)

〈Subscripts〉

P : grid node loaction at the center of the domain or Pressure
N : grid node at north
S : grid node at south
E : grid node at east
W : grid node at west
T : time step node
D : diffusion
l : laminar
t : turbulent

Referernce

1. Albright L.D. 1984. Building environmental control. AE682 Lecture Notebook, Conrell University, Ithaca, NY.
2. Barber E.M. 1981. Scale-model study of incomplete mixing in a ventilated air space. Unpublished Ph.D. Thesis, University of Guelph.
3. Boon, C.R. 1978. Airflow patterns and temperature distribution in an experimental piggery. JAER 23(2) : 129-139.
4. Boon, C.R. 1984. The control of climate environment for finishing pigs using lower critical temperature. JAER 29 : 295-303.
5. Carpenter, G.A.,L.J. Mousley Ⅶ J.M.Randall. 1972. Ventilation investigation using a section of a livestock building and air flow visualization by bubbles. JAER 17(4) : 323-331.
6. Carpenter, G.A.,L.J. Mousley. 1978. Resistance to airflow of materials used in ventilating livestock build ings. JAER 23 : 441-451.
7. Choi, Hong-Lim. 1989. Ventilation of agricultural structures. Daegwang Pub.
8. Choi, Hong-Lim & Suh. Won-Myung. 1988. Determination of environmental parameters for agricultural production structures. J. Inst. Agr. Res. Util. Gyeongsang Nat'l University 22(2) : 221.
9. Choi, Hong-Lim, Hyeon-Tae Kim, & Woo-Joong, Kim. 1991. Development of new conceptual ventilation graphs for mechanically ventilated livestock buildings. Trans. of KSAE 33(3) : 91-100.
10. Choi, Hong-Lim, L.D. Albright, M.B.Timmons & Z.Warhaft. 1988. An application of the k-ε turbulence model to predict air distribution in a slot-ventilated enclosure. Transaction. ASAE 31(6) : 1804-1814.
11. Choi, Hong-Lim, L.D. Albright & M.B. Timmons. 1990. An application of the k-ε turbulence model to predict how a rectangular opbstacle in a slot-ventilated enclosure affects air flow. Transaction. ASAE 33(1) : 274-281.
12. Hellickson M.A. & J.N. Walker(editors). 1983. Ventilation of agricultural structures. ASAE Monograph No.6. St.Joseph, MI.
13. Patankar, P.V. 1980. Numerical heat transfer and fluid flow. McGraw-Hill Book Company. NY.
14. Pattie,D.R. & W.R. Milne. 1966. Ventilation air flow patterns by using of models. Transaction ASAE 9(5) : 646-649.
15. Randall, J.M. 1975. The prediction of air flow patterns in a livestock building. JAER 20(2) : 199-215.
16. Randall, J.M & V.A. Battams. 1976. The observed influence of surface obstructions on the airflow pattern within livestock building. JAER 21(1) : 33-39.
17. Randall, J.M. 1979. The stability criteria for airflow patterns in livestock buildings. JAER 24 : 361-374.
18. Rodi, W. 1984. Turbulence models and their applications in hydraulics-A state of the art review.(1st ed.). International Association for Hydraulic Research, Delft.
19. Tennekes, H. & J.L. Lumley. 1972. A first course in turbulence. MIT Press, Cambridge, MA.
20. Timmons, M.B. 1979. Experimental and numerical study of air movement in slot-ventilated enclosures. Unpublished Ph.D. Thesis, Cornell University.
21. Timmons, M.B. 1984. Internal air velocity as affected by the size and location of continuous inlet slots. Transaction ASAE 27(5) : 1514-1517.